Check for updates

Geophysical Research Letters

RESEARCH LETTER
10.1029/2024GL110220

A Slowdown in Translation Speed of Western North Pacific Tropical Cyclones Undergoing Rapid Intensification

Jinjie Song[1,2], **Philip J. Klotzbach**[3], **Yifei Dai**[1,2], **and Yihong Duan**[2]

[1]Nanjing Joint Institute for Atmospheric Sciences, Chinese Academy of Meteorological Sciences, Nanjing, China, [2]State Key Laboratory of Severe Weather, Chinese Academy of Meteorological Sciences, Beijing, China, [3]Department of Atmospheric Science, Colorado State University, Fort Collins, CO, USA

Key Points:

- There is a significant slowdown in the mean translation speed of western North Pacific tropical cyclones undergoing rapid intensification
- Slow-moving (fast-moving) tropical cyclones have a significant increasing (virtually unchanged) rapid intensification probability
- A deepening of the western North Pacific mixed layer is the primary driver of the deceleration of rapid intensification cases

Correspondence to:
J. Song,
songjinjie@qq.com

Citation:
Song, J., Klotzbach, P. J., Dai, Y., & Duan, Y. (2024). A Slowdown in translation speed of western North Pacific tropical cyclones undergoing rapid intensification. *Geophysical Research Letters*, *51*, e2024GL110220. https://doi.org/10.1029/2024GL110220

Received 9 MAY 2024
Accepted 11 SEP 2024

Abstract This study examines long-term trends in western North Pacific (WNP) tropical cyclones (TCs) experiencing rapid intensification (RI) from 1971 to 2022. Although there is only a weak slowdown for all intensifying WNP TCs, the average translation speed for RI TCs has significantly decelerated over the RI main development region (7.5°–25°N, 115°–160°E). This slowdown is primarily due to increasing RI probabilities for slower-moving TCs. By contrast, the RI probability of faster-moving TCs remains virtually unchanged. These differences in RI trend probabilities between slow-moving and fast-moving TCs are primarily linked to a deepening of the WNP mixed layer. TC-induced sea surface temperature cooling tends to weaken when the mixed layer is deep. During the intensification stage, the deeper mixed layer is more critical for slower-moving TCs than for faster-moving TCs. Our findings suggest that RI probabilities for slow-moving WNP TCs may continue to increase in a future warming climate.

Plain Language Summary Rapid intensification (RI) poses a considerable challenge for operational tropical cyclone (TC) forecasting. Several studies have found increasing trends in RI frequency, ratio and magnitude over the western North Pacific (WNP) during recent decades. This study focuses on the translation speed for WNP TCs experiencing RI from 1971 to 2022. The average movement of RI TCs has significantly decelerated over the RI main development region, where a majority of RI cases occur climatologically. This slowdown is primarily induced by significantly increasing RI probabilities for slower-moving TCs and virtually unchanged RI probabilities for faster-moving TCs. These differences in RI probabilities between slower-moving and faster-moving TCs cannot be explained by weak changes in the steering flow or favorability of the thermodynamic environment over the WNP. Instead, these results are primarily linked to a deepening of the WNP mixed layer. TC-induced sea surface temperature cooling tends to weaken when the mixed layer is deep. Previous idealized simulations have shown that a deeper mixed layer is more critical to TC intensification for slower-moving TCs than for faster-moving TCs. Our findings suggest that RI probabilities for slow-moving WNP TCs may continue to increase in a future warming climate.

1. Introduction

Rapid intensification (RI) is classified as a rapid increase in tropical cyclone (TC) intensity during a short time period. RI is often identified when a TC maximum sustained wind speed increases by at least 30 kt in a 24-hr interval (e.g., Kaplan & DeMaria, 2003). Forecast models still struggle at accurately predicting RI, posing considerable challenges for operational TC forecasting (Knaff et al., 2018). Given increasing concerns about global warming and its impacts on TC activity, there has been heightened focus on long-term RI trends (Intergovernmental Panel on Climate Change, 2023).

Several studies have examined long-term changes in various RI metrics over the western North Pacific (WNP), which climatologically has more frequent RI occurrences than any other TC ocean basin (Lee et al., 2016). Over the WNP, although the number of RI events occurring in offshore regions (e.g., within 400 km of the coast) has significantly increased during recent decades (Li et al., 2023), there is no obvious long-term trend in basinwide RI frequency (Kang & Elsner, 2019; Wang et al., 2015). By contrast, the annual proportion of RI records to total TC records over the whole WNP basin has exhibited a significant increasing trend since the early 1980s (Bhatia et al., 2019, 2022). There has also been a significant increase in annual WNP RI magnitude, which is linked to a significantly increasing number of strong RI events, defined as 24-hr TC intensity increases of at least 50 kt (Song et al., 2020). These trends imply enhanced WNP RI activity, driven by more favorable thermodynamic

© 2024. The Author(s).
This is an open access article under the terms of the Creative Commons Attribution License, which permits use, distribution and reproduction in any medium, provided the original work is properly cited.

19448007, 2024, 18, Downloaded from https://agupubs.onlinelibrary.wiley.com/doi/10.1029/2024GL110220, Wiley Online Library on [12/02/2025]. See the Terms and Conditions (https://onlinelibrary.wiley.com/terms-and-conditions) on Wiley Online Library for rules of use; OA articles are governed by the applicable Creative Commons License

environments for TC intensification (e.g., the warming ocean) (Bhatia et al., 2019, 2022; Li et al., 2023; Song et al., 2020).

Kossin (2018) noted a significant slowdown of TC motion over the WNP during 1949–2016. This tendency was questioned in Moon et al. (2019) and Lanzante (2019) given the low reliability of TC best track data during the pre-satellite era before the 1970s. When focusing on the satellite era, several studies (e.g., Chan, 2019; Kim et al., 2020; Sun et al., 2021; Wang et al., 2020) have found a weak and insignificant trend in basin-averaged TC translation speed over the WNP. However, a robust slowing of TC motion was reported over some sub-regions of the WNP. Yamaguchi et al. (2020) and Zhang, Zhang, et al. (2020) both projected decreasing WNP TC translation speeds at higher latitudes in a warmer climate, consistent with a slowing steering flow caused by a poleward shift of the midlatitude westerlies. Wu et al. (2022) observed a slowdown in landfalling TC motion over South China, which they attributed to an anomalous cyclonic circulation over the western WNP that acted to slow the climatological northwestward steering flow.

Numerous previous publications have noted that TC translation speed positively correlates with TC intensity and TC intensity changes (e.g., Lin, Pun, & Wu, 2009; Mei et al., 2012; Walker et al., 2014; Y. Wang and Wu, 2004; Zhao & Chan, 2017). The passage of a TC can induce sea surface temperature (SST) cooling that is unfavorable for additional TC development via vertical mixing and upwelling. Vertical mixing is induced by turbulence generated by the TC's surface winds, which entrains cold water at lower levels into the mixed layer. Upwelling also results from Ekman pumping forced by the cyclonic flow generated by the TC's surface winds. Faster-moving (slower-moving) TCs tend to generate weaker (stronger) sea surface cooling and have shorter (longer) exposure to the cooling, leading to a weakened (strengthened) negative SST feedback.

Sun et al. (2021) showed that the global TC slowdown tended to be greater for stronger TCs, with a slowdown rate that approximately doubled if tropical depressions were excluded. Nonetheless, stronger WNP TCs did not exhibit a significant slowdown trend during the satellite era. To this point, it remains unclear whether there is a relationship between WNP TC intensity change and TC translation speed. This study therefore investigates how the translation speed of WNP RI cases has changed during the past ∼5 decades.

The remainder of this study is organized as follows. Section 2 introduces the TC and environmental datasets employed as well as the methodology used for the analysis. Section 3 examines the climatology and trends in translation speeds between RI cases and all cases over the WNP. Section 4 discusses trends in both atmospheric and oceanic conditions as well as their potential influences on changes in translation speeds for RI events. This study concludes with a summary in Section 5.

2. Data and Methods

This study applies 6-hourly TC best track data from the Joint Typhoon Warning Center (JTWC) as archived in the International Best Track Archive for Climate Stewardship (IBTrACS) v04r00 (Knapp et al., 2010). Given inconsistent and changing measurement technologies and reporting practices, systematic overestimates in TC intensity existed in the JTWC data during the pre-satellite era (Emanuel, 2000). Hence this study focuses on the period of 1971–2022, as an increasing fraction of intensities have been estimated through satellite observation since the 1970s (Emanuel, 2000). We only consider 6-hr TC cases with an intensity of at least 34 kt (e.g., named storms), in order to reduce the uncertainty in detecting weak TCs such as tropical depressions (Klotzbach & Landsea, 2015). Similar to previous RI-related publications (Kaplan & DeMaria, 2003; Kaplan et al., 2010; Knaff et al., 2018; Shimada et al., 2020; Shu et al., 2012), an RI case is identified as a 24-hr V_{max} (ΔV_{24}) intensification of at least 30 kt over water, approximately corresponding to the 95th percentile of ΔV_{24} for all TC cases. Starting from the first 6-hr point (t_0) of the TC, a ΔV_{24} ($V_{max}[t_0 + 24\ hr] - V_{max}[t_0]$) is calculated for every 6-hr point. Accordingly, the translation speed is computed as the great-circle distance between the TC centers at t_0 and $t_0 + 24$ hr divided by 24 hr.

Figure 1a displays the spatial patterns of the climatological average 24-hr intensification rate, which is computed as the mean ΔV_{24} for TCs experiencing an intensification stage ($\Delta V_{24} > 0$ kt) in each 5° × 5° grid. Figure 1b shows the accumulated RI occurrence number during 1971–2022. A majority (89%) of RI cases occur over the region spanning 7.5°–25°N, 115°–160°E [hereafter the RI main development region (MDR)], where the average intensification rates are generally higher than over other regions. Our results that follow are not significantly changed when using other RI MDR definitions (e.g., Fudeyasu et al., 2018; Wang et al., 2015; B. Wang and

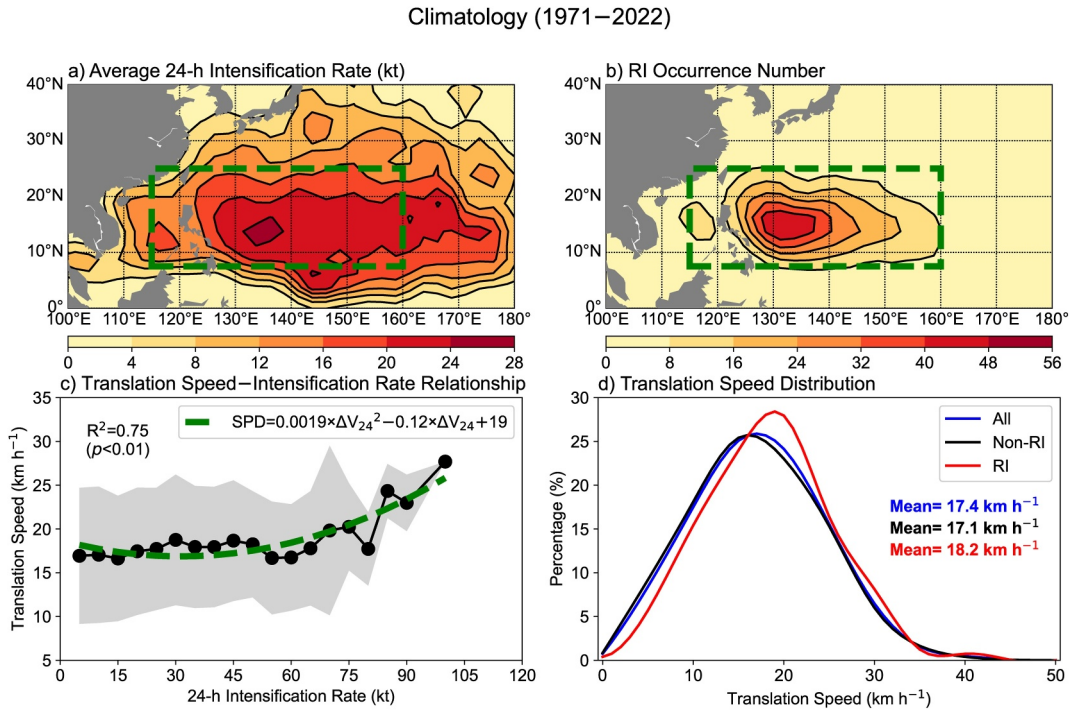

Figure 1. (a), (b) Climatological (a) average 24-hr intensification rate and (b) RI occurrence number over the WNP during 1971–2022. The dashed green box denotes the RI main development region (MDR; 7.5°–25°N, 115°–160°E). (c) Average translation speed for 6-hr TC records over the RI MDR as a function of the simultaneous 24-hr intensification rate. The shading indicates ±1 standard deviation. The green dashed line is obtained through least squares regression, while its explained variance and the corresponding significance level are shown in the panel. (d) Translation speed distributions for all, non-RI and RI cases over the RI MDR. The mean translation speeds for different groups are given in the panel.

Zhou, 2008; Zhang, Murakami, et al., 2020). The RI MDR identified here is consistent with that shown in previous studies (e.g., Fudeyasu et al., 2018; Shu et al., 2012; B. Wang and Zhou, 2008). This study thus focuses on changes in TC activity and the large-scale environment over the RI MDR.

Monthly mean atmospheric variables are obtained from the fifth generation European Center for Medium-Range Weather Forecasts (ECMWF) reanalysis of the global climate (ERA5; Hersbach et al., 2020) with a resolution of 0.25° × 0.25°. Monthly mean SST data over a 1° × 1° grid are downloaded from the Hadley Center Sea Ice and Sea Surface Temperature dataset (HadISST; Rayner et al., 2003). Monthly ocean temperature profiles and depths of the mixed layer and the 26°C isotherm are from the control member of the ECMWF Ocean Reanalysis System 5 (ORAS5; Zuo et al., 2019) on a 0.25° × 0.25° grid. HadISST and ERA5 provide the primary forcing fields for ORAS5 (Zuo et al., 2019), leading to physical consistency between these datasets.

For our analysis on shorter timescales, we use 6-hr atmospheric variables and SSTs provided by ERA5. Daily ocean temperature profiles from 1971 to 2016 are obtained from the Ocean General Circulation Model for the Earth Simulator version 2 (OFES2; Sasaki et al., 2020) at a horizontal resolution of 0.1° × 0.1°. These profiles are then temporally interpolated to a 6-hr interval.

Previous studies (e.g., Fudeyasu et al., 2018; Knaff et al., 2018; Shu et al., 2012) have suggested that several factors can influence RI activity, including SST, TC heat potential (TCHP), 700–500-hPa relative humidity, 850-hPa relative vorticity, 200-hPa divergence and 850–200-hPa vertical wind shear (VWS). The long-term trends in these indices are based on monthly data. These trends are not significantly changed if we use 6-hr data after excluding the days when at least one TC occurred over the WNP. In addition, for individual 6-hr TC cases, the aforementioned environmental factors are calculated by averaging over the circular region within 200–800 km from the TC center, to minimize the influence of the TC itself (e.g., DeMaria et al., 2005).

This study uses a two-tailed Student's *t*-test to estimate significance levels (p) of correlation coefficients (r), linear trends and the differences in means between the two samples.

19448007, 2024, 18, Downloaded from https://agupubs.onlinelibrary.wiley.com/doi/10.1029/2024GL110220, Wiley Online Library on [12/02/2025]. See the Terms and Conditions (https://onlinelibrary.wiley.com/terms-and-conditions) on Wiley Online Library for rules of use; OA articles are governed by the applicable Creative Commons License

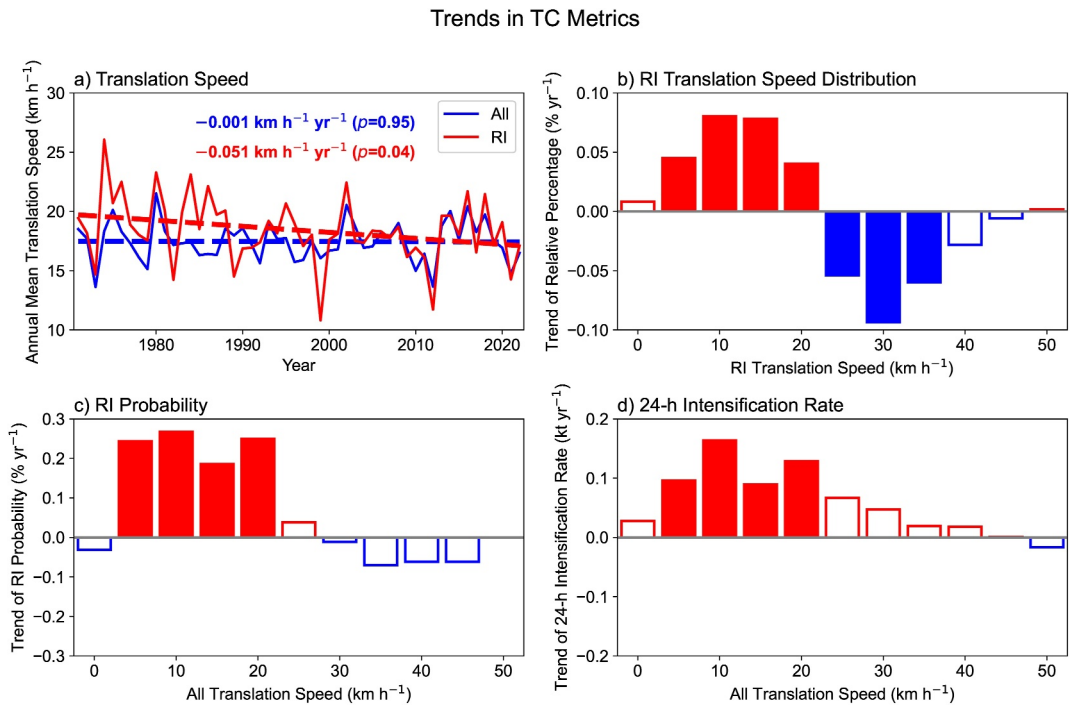

Figure 2. (a) Annual changes in mean translation speeds for all cases and RI cases during 1971–2022. The dashed lines denote the long-term trends obtained by least squares, while their corresponding slopes and significance levels are shown in the panel. (b)–(d) Long-term changes in (b) the translation speed distribution for RI cases, (c) the RI probability for TCs with different translation speeds and (d) the average 24-hr intensification rate for TCs with different translation speeds during 1971–2022. Trends significant at the 0.05 level are displayed as color-filled bars.

3. Trends in RI Translation Speed

There is a weak but significant correlation between the TC 24-hr intensification rate and the simultaneous translation speed ($r = 0.06$; $p < 0.01$), consistent with the positive relationship noted in previous studies (e.g., Lin, Pun, & Wu, 2009; Mei et al., 2012; Walker et al., 2014; Y. Wang and Wu, 2004; Zhao & Chan, 2017). Figure 1c shows that the relationship is nonlinear. The average translation speed shows less change for $\Delta V_{24} < 60$ kt, while it increases more notably for storms intensifying at extremely rapid rates ($\Delta V_{24} \geq 60$ kt). This means that the positive relationship between intensification rate and translation speed is more significant for RI cases. Figure 1d presents the translation speed distributions for all intensification cases ($\Delta V_{24} > 0$ kt), non-RI cases (0 kt $< \Delta V_{24} <$ 30 kt) and RI cases over the RI MDR. The distributions for all cases and non-RI cases are almost identical, given the large proportion of non-RI cases to all cases (6,832 out of 8,850). By contrast, the distribution for RI cases generally migrates toward greater translation speeds. The mean translation speed for RI cases is ~1 km hr^{-1} larger than that for all cases and non-RI cases. This difference is significant at the 0.05 level.

Figure 2a displays variations in annual mean translation speeds for all cases and RI cases during 1971–2022. There is a significant positive correlation ($r = 0.61$; $p < 0.01$), meaning that both have similar influencing factors on interannual timescales. There is a weak and insignificant slowdown in the mean translation speed for all TC cases, consistent with previous studies (e.g., Chan, 2019; Kim et al., 2020; Sun et al., 2021; Wang et al., 2020). However, the translation speed for RI cases significantly decreases at a rate of −0.051 km hr^{-1} yr^{-1} ($p = 0.04$), which is one order of magnitude larger than the slowing trend for all cases. This implies that the slowdown tends to be greater for TCs with higher intensification rates. Figure 2b further illustrates long-term changes in the translation speed distribution for RI cases during 1971–2022. The aforementioned slowdown in the mean translation speed corresponds to an increasing proportion of slower-moving RI events and a decreasing proportion of faster-moving RI events.

Figures 2c and 2d show trends in RI probability and average ΔV_{24}, respectively, for TCs with different translation speeds during 1971–2022. There are significant increases in RI probability for TCs with a

19448007, 2024, 18, Downloaded from https://agupubs.onlinelibrary.wiley.com/doi/10.1029/2024GL110220, Wiley Online Library on [12/02/2025]. See the Terms and Conditions (https://onlinelibrary.wiley.com/terms-and-conditions) on Wiley Online Library for rules of use; OA articles are governed by the applicable Creative Commons License

translation speed of 5–20 km hr^{-1} and weak decreases in RI probability for TCs moving faster than 25 km hr^{-1} (Figure 2c). This highlights that slower-moving TCs have an increased opportunity to undergo RI, while the RI probability for faster-moving TCs remains almost unchanged. This also means that the shift of the RI translation speed distribution as displayed in Figure 2b tends to be primarily caused by an increasing frequency of slower-moving RI events. Similarly, compared with faster-moving TCs, slower-moving TCs generally exhibit a larger increasing trend in average ΔV_{24}, meaning a greater chance of intensification (Figure 2d). There are strong and significant increases in average ΔV_{24} for TCs with a translation speed of 5–20 km hr^{-1} but weak and insignificant decreases in the average ΔV_{24} for TCs moving faster than 20 km hr^{-1}.

4. Trends in Environmental Conditions

This study focuses on environmental changes from July–November, which includes 84% of RI events that occurred during the entire year (Ge et al., 2018; B. Wang and Zhou, 2008). Figure 3a displays the trend in the 850–300-hPa steering flow from 1971 to 2022. There are almost no significant changes in the steering flow over the tropical WNP, with significant easterly anomalies observed at higher latitudes. This is consistent with our finding of insignificant changes in translation speed for all TC cases over the RI MDR. This also implies that the significant slowdown of RI events cannot be explained by steering flow changes.

Figures 3b–3g presents trends in environmental conditions that have been previously shown to impact WNP RI activity. Consistent with Song et al. (2021) and Klotzbach et al. (2022), there are significant increasing trends in thermodynamic variables (e.g., SST, TCHP and 700–500-hPa relative humidity) over the RI MDR during 1971–2022. These more favorable thermodynamic conditions all enhance TC intensification and favor RI occurrence (Figures 3b–3d). Significant increases in SST and TCHP occur over almost the entire MDR, while significant increases in relative humidity are concentrated over the southwestern part of the MDR. By contrast, there are no significant changes in dynamic variables (e.g., 850-hPa relative vorticity, 200-hPa divergence and 850–200-hPa VWS) over most of the WNP, except significant decreases in divergence near the southwestern edge of the MDR (Figures 3e–3g). These results confirm that the warming ocean is the major contributor to enhanced RI activity during recent decades, as noted by Bhatia et al. (2019), Song et al. (2020), Bhatia et al. (2022) and Li et al. (2023).

In addition, Figure 4 displays changes in environmental conditions for 6-hr TC cases over the RI MDR. We separate these cases into slow-moving and fast-moving groups using a translation speed threshold of 22.5 km hr^{-1}, corresponding to different changes in RI probability as shown in Figure 2c. Regardless of TC translation speed, thermodynamic conditions (e.g., SST, TCHP, and humidity) become significantly more favorable for TC intensification (Figures 4a–4f). By contrast, dynamic conditions (e.g., vorticity, divergence and VWS) change insignificantly (Figures 4g–4l). These changes in 6-hr TC-surrounding environmental conditions are consistent with the trends in July–November mean conditions as displayed in Figures 3b–3g. This implies that slow-moving TCs do not have a more favorable environment for intensification than fast-moving TCs.

If more RI-favorable environmental conditions were the main factor leading to the slower movement of RI cases, the RI proportion of TCs would become greater regardless of translation speed. However, significant RI ratio increases are only observed for slow-moving TCs (Figure 2c). Over the RI MDR, significant increases in ocean temperature are found between the surface and ~100-m depth, corresponding to a global warming signal in the ocean (Figure 5a). Consistent with Figures 3b and 3c, the RI MDR-averaged SST and TCHP both have significantly increased from 1971 to 2022 (Figures 5b and 5c). Given the warming of subsurface water, the 26°C isotherm now extends to a significantly deeper depth (Figure 5d).

Moreover, above 100-m depth, the warming rate of the ocean temperature increases with depth, meaning a decreasing vertical temperature gradient (Figure 5a). As a result, there is a significant deepening of the mixed layer over the RI MDR, with a rate of 0.078 m yr^{-1} ($p < 0.01$) (Figure 5e). When using the daily OFES2 dataset, there is also a significant increasing trend in mixed layer depth during 1971–2016, with a rate of 0.053 m yr^{-1} ($p < 0.01$). This trend changes only slightly to 0.051 m yr^{-1} ($p < 0.01$), if the days when at least one TC occurs over the WNP are excluded. This means that long-term changes in the mixed layer depth are not significantly influenced by TC activity.

19448007, 2024, 18, Downloaded from https://agupubs.onlinelibrary.wiley.com/doi/10.1029/2024GL110220, Wiley Online Library on [12/02/2025]. See the Terms and Conditions (https://onlinelibrary.wiley.com/terms-and-conditions) on Wiley Online Library for rules of use; OA articles are governed by the applicable Creative Commons License

10.1029/2024GL110220

19448007, 2024, 18, Downloaded from https://agupubs.onlinelibrary.wiley.com/doi/10.1029/2024GL110220, Wiley Online Library on [12/02/2025]. See the Terms and Conditions (https://onlinelibrary.wiley.com/terms-and-conditions) on Wiley Online Library for rules of use; OA articles are governed by the applicable Creative Commons License

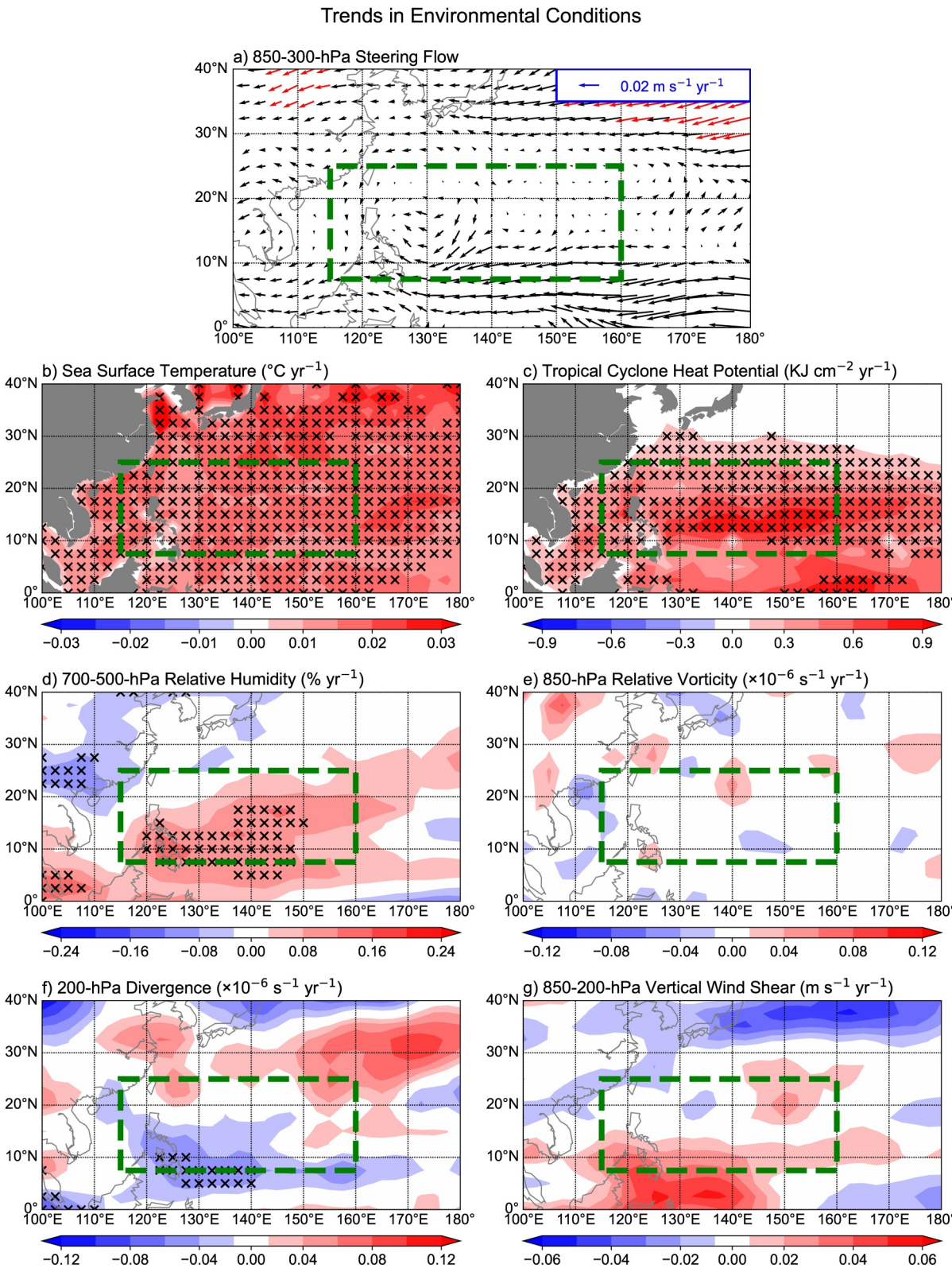

Figure 3. Trends in July–November mean (a) 850–300-hPa steering flow, (b) SST, (c) TCHP, (d) 700–500-hPa relative humidity, (e) 850-hPa relative vorticity, (f) 200-hPa divergence and (g) 850–200-hPa VWS from 1971 to 2022. Flow trends significant at the 0.05 level are shown as red vectors in (a), while slopes significant at the 0.05 level are denoted by black crosses in (b)–(g). Dashed green boxes denote the RI main development region (MDR; 7.5°–25°N, 115°–160°E).

10.1029/2024GL110220

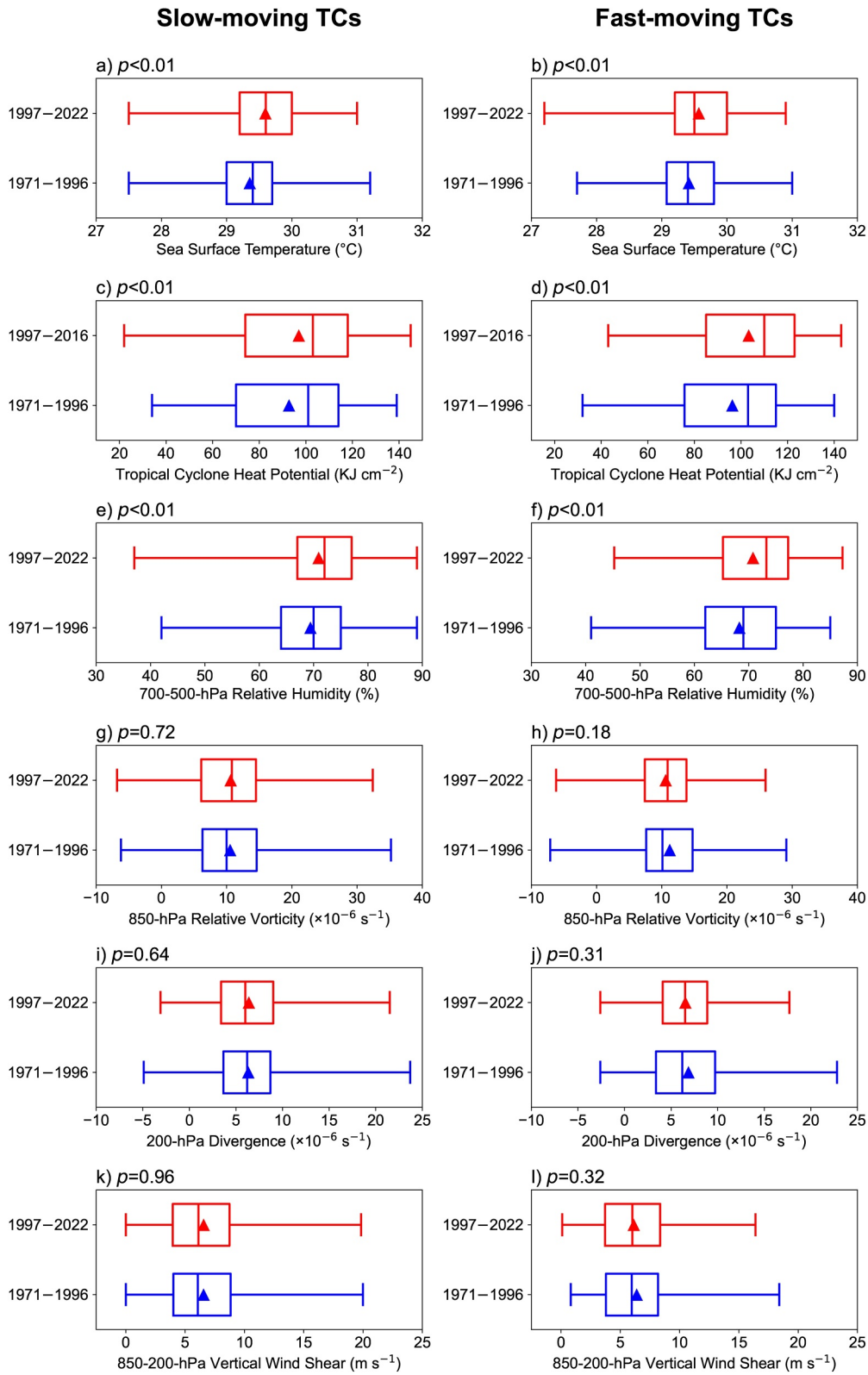

Figure 4. Boxplots of (a), (b) SST, (c), (d) TCHP, (e), (f) 700–500-hPa relative humidity, (g), (h) 850-hPa relative vorticity, (i), (j) 200-hPa divergence and (k, l) 850–200-hPa VWS for 6-hr TC cases occurring over the RI MDR during different periods. The left and right columns are for slow-moving TCs (translation speed <22.5 km hr^{-1}) and fast-moving TCs (translation speed ≥ 22.5 km hr^{-1}), respectively. The significance level of the difference between the means (triangles) is shown in the title of each panel.

19448007, 2024, 18, Downloaded from https://agupubs.onlinelibrary.wiley.com/doi/10.1029/2024GL110220, Wiley Online Library on [12/02/2025]. See the Terms and Conditions (https://onlinelibrary.wiley.com/terms-and-conditions) on Wiley Online Library for rules of use; OA articles are governed by the applicable Creative Commons License

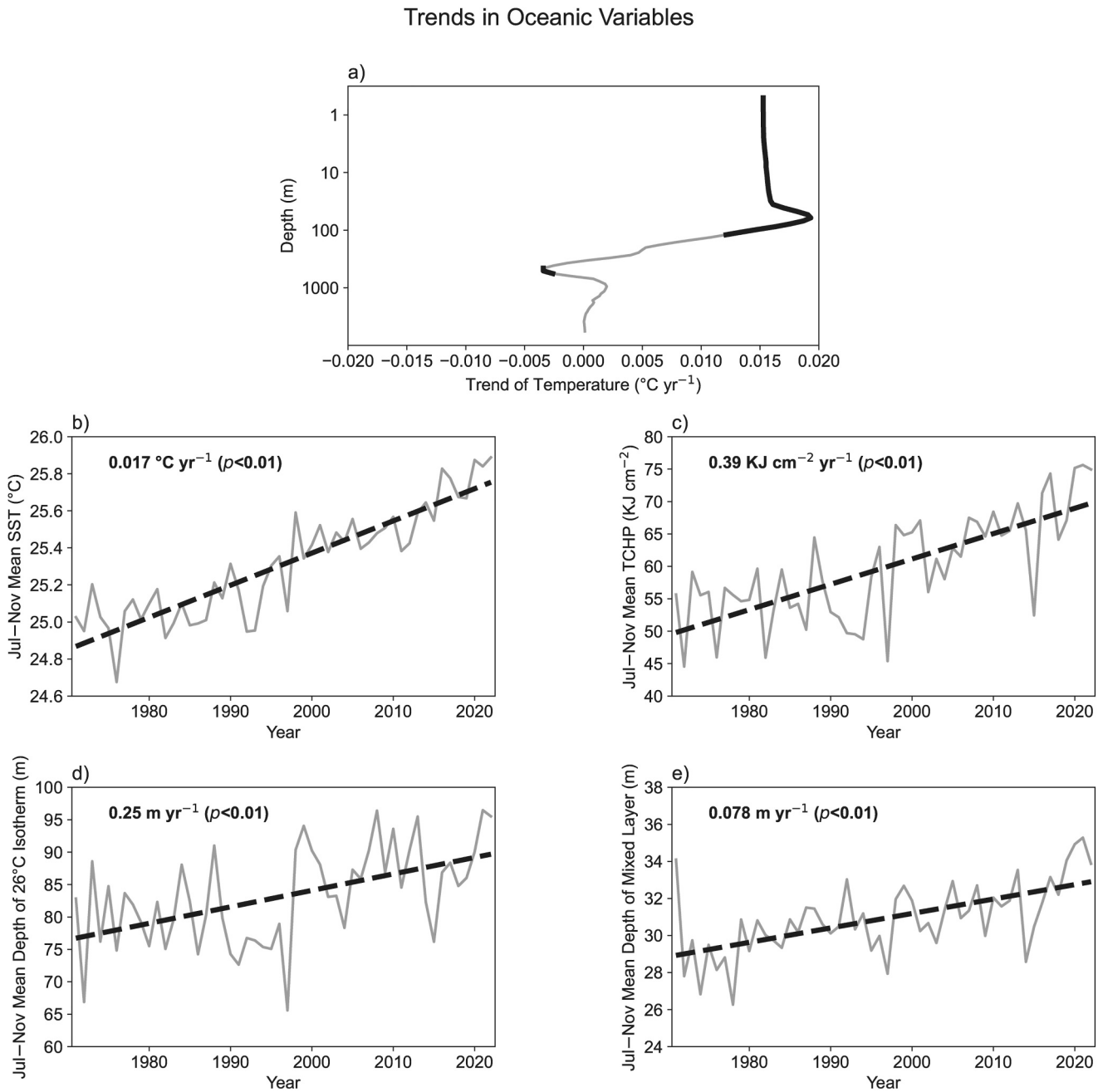

Figure 5. (a) Trends in ocean temperature at different depths over the RI MDR during July–November in 1971–2022. Thick lines denote trends significant at the 0.05 level. (b)–(e) Annual variations in (b) SST, (c) TCHP, (d) depth of 26°C isotherm and (e) depth of mixed layer averaged during July–November over the RI MDR from 1971 to 2022, as well as their long-term trends. The trend values and their significance levels are shown in the panels.

It is well accepted that there is an interaction between TCs and the underlying upper ocean (e.g., Emanuel, 2001; Emanuel et al., 2004). Changes in upper-ocean temperature can influence TC activity, while the passage of the TC can modulate the thermal and dynamical structure of the upper ocean. On one hand, TCs usually cool the surface ocean and warm the subsurface ocean, leading to a deepened mixed layer (Zhang et al., 2021). On the other hand, mixed layer depth significantly (marginally) affects various TC parameters (e.g., intensity, size and destructiveness) before (after) reaching a depth threshold that is mainly determined by TC intensity (Zhang et al., 2024). Nonetheless, this interaction between TCs and the upper ocean is primarily

19448007, 2024, 18, Downloaded from https://agupubs.onlinelibrary.wiley.com/doi/10.1029/2024GL110220, Wiley Online Library on [12/02/2025]. See the Terms and Conditions (https://onlinelibrary.wiley.com/terms-and-conditions) on Wiley Online Library for rules of use; OA articles are governed by the applicable Creative Commons License

19448007, 2024, 18, Downloaded from https://agupubs.onlinelibrary.wiley.com/doi/10.1029/2024GL110220, Wiley Online Library on [12/02/2025]. See the Terms and Conditions (https://onlinelibrary.wiley.com/terms-and-conditions) on Wiley Online Library for rules of use; OA articles are governed by the applicable Creative Commons License

observed on synoptic or weekly timescales, because TC-induced temperature anomalies in the upper ocean typically disappear over a timescale of a couple of weeks (Dare & McBride, 2011; Ma et al., 2020; Mei & Pasquero, 2013; Price et al., 2008). On interannual or longer timescales, there is only a minor impact of TCs on the upper ocean. By analyzing observations and conducting numerical simulations, Wu et al. (2018) reported a dominant role of the mixed layer depth in the increasing ratio of the most intense TCs over the WNP during recent decades.

Several studies have also investigated the role of the mixed layer depth in simulating RI for TC cases (e.g., Lin, Chen, et al., 2009; Sun et al., 2016; Wang et al., 2018; Yesubabu et al., 2020). The common conclusion is that a deeper mixed layer is generally associated with higher TCHP, which favors RI of simulated TCs, including faster RI onset and longer RI duration. By contrast, TCs intensify at a slower rate and are less likely to experience RI when a shallower mixed layer is considered.

By using an idealized atmosphere-ocean coupled model, Zhao and Chan (2017) found that the simulated TC-induced SST cooling became weaker when an initial deeper mixed layer was given. The weakening magnitude was much more evident for slow-moving TCs than for fast-moving TCs. As a consequence, when the mixed layer depth increased, there was a weakening negative feedback of TC-induced SST cooling for slow-moving TCs. By comparison, the change in SST cooling tended to be negligible for fast-moving TCs. We find that the deeper mixed layer is likely the reason why only the slower-moving TCs have shown an increasing chance of undergoing RI.

5. Summary

Long-term changes in translation speed of WNP TCs experiencing RI and their related mechanisms are investigated in this study. Climatologically, there is a significant positive correlation between 24-hr intensity change and simultaneous translation speed. RI events generally exhibit faster translation speeds than other intensification cases. Consistent with previous publications (e.g., Chan, 2019; Kim et al., 2020; Sun et al., 2021; Wang et al., 2020), there is only a weak slowdown for all intensification cases over the WNP during 1971–2022. However, there is a significant slowdown in RI cases over the MDR (7.5°–25°N, 115°–160°E). This is primarily caused by significant increases in the RI probability for slow-moving TCs.

The 850–300-hPa steering flow shows no significant trend over the MDR, implying that it plays only a minor role in the slowdown of RI events. As noted in previous studies (e.g., Bhatia et al., 2019; Bhatia et al., 2022; Li et al., 2023; Song et al., 2020), there is a more RI-favorable thermodynamic environment over the MDR, including higher SST, larger TCHP and a moister troposphere. Although these environmental changes have been found to contribute to enhanced WNP RI activity, we primarily link the slowdown in RI cases to the deepening of the ocean mixed layer over the MDR. When the mixed layer is deeper, the TC-induced SST cooling weakens, with the effect of this weakened SST cooling being much stronger for slower-moving TCs (Zhao & Chan, 2017). This explains why slower-moving TCs have an increasing chance of undergoing RI, while the RI probability of faster-moving TCs shows little change.

Our results highlight distinct trends in the translation speed of WNP TCs with different intensification rates during recent decades. Our findings suggest that more attention should be paid to the RI probability of slow-moving TCs in operational forecasting. We intend to verify these results using numerical projections from high-resolution climate models in future work.

Data Availability Statement

All data used in this study are freely available online. Western North Pacific TC Best track data are obtained from Knapp et al. (2018). The Hadley Centre Sea Ice and Sea Surface Temperature (HadISST) data are downloaded from the Hadley Centre for Climate Prediction and Research/Met Office/Ministry of Defence/United Kingdom (2000). The fifth generation European Centre for Medium-Range Weather Forecasts (ECMWF) atmospheric reanalysis of the global climate (ERA5) data are retrieved from Hersbach et al. (2017). The ECMWF Ocean Reanalysis System 5 (ORAS5) data are provided by Copernicus Climate Change Service/Climate Data Store (2021). The Ocean General Circulation Model for the Earth Simulator version 2 (OFES2) data are provided by JAMSTEC (2009).

Acknowledgments
This work was jointly funded by the National Natural Science Foundation of China (U2342203, 42192554, 61827901, 42175007, 41905001, and 42192552). Klotzbach would like to acknowledge financial support from the G. Unger Vetlesen Foundation.

References

Bhatia, K., Baker, A., Yang, W., Vecchi, G., Knutson, T., Murakami, H., et al. (2022). A potential explanation for the global increase in tropical cyclone rapid intensification. *Nature Communications*, *13*(1), 6626. https://doi.org/10.1038/s41467-022-34321-6

Bhatia, K. T., Vecchi, G. A., Knutson, T. R., Murakami, H., Kossin, J., Dixon, K. W., & Whitlock, C. E. (2019). Recent increases in tropical cyclone intensification rates. *Nature Communications*, *10*(1), 635. https://doi.org/10.1038/s41467-019-08471-z

Chan, K. T. F. (2019). Are global tropical cyclones moving slower in a warming climate? *Environmental Research Letters*, *14*(10), 104015. https://doi.org/10.1088/1748-9326/ab4031

Copernicus Climate Change Service/Climate Data Store. (2021). ORAS5 global ocean reanalysis monthly data from 1958 to present [Dataset]. *Copernicus Climate Change Service (C3S) Climate Data Store (CDS)*. https://doi.org/10.24381/cds.67e8eeb7

Dare, R. A., & McBride, J. L. (2011). Sea surface temperature response to tropical cyclones. *Monthly Weather Review*, *139*(12), 3798–3808. https://doi.org/10.1175/mwr-d-10-05019.1

DeMaria, M., Mainelli, M., Shay, L. K., Knaff, J. A., & Kaplan, J. (2005). Further improvements to the statistical hurricane intensity prediction Scheme (SHIPS). *Weather Forecasting*, *20*(4), 531–543. https://doi.org/10.1175/waf862.1

Emanuel, K. A. (2000). A statistical analysis of tropical cyclone intensity. *Monthly Weather Review*, *128*(4), 1139–1152. https://doi.org/10.1175/1520-0493(2000)128<1139:asaotc>2.0.co;2

Emanuel, K. A. (2001). Contribution of tropical cyclones to meridional heat transport by the oceans. *Journal of Geophysical Research*, *106*(D14), 14771–14781. https://doi.org/10.1029/2000jd900641

Emanuel, K. A., DesAutels, C., Holloway, C., & Korty, R. (2004). Environmental control of tropical cyclone intensity. *Journal of the Atmospheric Sciences*, *61*(7), 843–858. https://doi.org/10.1175/1520-0469(2004)061<0843:ecotci>2.0.co;2

Fudeyasu, H., Ito, K., & Miyamoto, Y. (2018). Characteristics of tropical cyclone rapid intensification over the western North Pacific. *Journal of Climate*, *31*(21), 8917–8930. https://doi.org/10.1175/jcli-d-17-0653.1

Ge, X., Shi, D., & Guan, L. (2018). Monthly variations of tropical cyclone rapid intensification ratio in the western North Pacific. *Atmospheric Science Letters*, *9*(4), e814. https://doi.org/10.1002/asl.814

Hadley Centre for Climate Prediction and Research/Met Office/Ministry of Defence/United Kingdom. (2000). Hadley Centre global Sea Ice and Sea Surface temperature (HadISST) [dataset]. *Research Data Archive at the National Center for Atmospheric Research, Computational and Information Systems Laboratory*. https://doi.org/10.5065/XMYE-AN84

Hersbach, H., Bell, B., Berrisford, P., Hirahara, S., Horányi, A., Muñoz-Sabater, J., et al. (2020). The ERA5 global reanalysis. *Quarterly Journal of Royal Meteorological Society*, *146*(730), 1999–2049. https://doi.org/10.1002/qj.3803

Hersbach, H., Bell, B., Berrisford, P., Hirahara, S., Horányi, A., Muñoz-Sabater, J., et al. (2017). Complete ERA5 from 1940: Fifth generation of ECMWF atmospheric reanalyses of the global climate [Dataset]. *Copernicus Climate Change Service (C3S) Data Store (CDS)*. https://doi.org/10.24381/cds.143582cf

Intergovernmental Panel on Climate Change. (2023). Weather and climate extreme events in a changing climate. In *Climate change 2021 – the physical science basis: Working group I contribution to the Sixth Assessment Report of the Intergovernmental panel on climate change* (pp. 1513–1766). Cambridge University Press.

JAMSTEC. (2009). JAMSTEC OFES (Ocean General circulation model for the Earth simulator) dataset [dataset]. *JAMSTEC*. https://doi.org/10.17596/0002029

Kang, N., & Elsner, J. B. (2019). Influence of global warming on the rapid intensification of western North Pacific tropical cyclones. *Environmental Research Letters*, *14*(4), 044027. https://doi.org/10.1088/1748-9326/ab0b50

Kaplan, J., & DeMaria, M. (2003). Large-scale characteristics of rapidly intensifying tropical cyclones in the North Atlantic Basin. *Weather and Forecasting*, *18*(6), 1093–1108. https://doi.org/10.1175/1520-0434(2003)018<1093:lcorit>2.0.co;2

Kaplan, J., DeMaria, M., & Knaff, J. A. (2010). A revised tropical cyclone rapid intensification index for the Atlantic and east Pacific basins. *Weather Forecasting*, *25*(1), 220–241. https://doi.org/10.1175/2009waf2222280.1

Kim, S. –H., Moon, I. –J., & Chu, P. –S. (2020). An increase in global trends of tropical cyclone translation speed since 1982 and its physical causes. *Environmental Research Letters*, *15*(9), 094084. https://doi.org/10.1088/1748-9326/ab9e1f

Klotzbach, P. J., & Landsea, C. W. (2015). Extremely intense hurricanes: Revisiting Webster et al. (2005) after 10 years. *Journal of Climate*, *28*(19), 7621–7629. https://doi.org/10.1175/jcli-d-15-0188.1

Klotzbach, P. J., Wood, K. M., Schreck, C. J., Bowen, S. G., Patricola, C. M., & Bell, M. M. (2022). Trends in global tropical cyclone activity: 1990–2021. *Geophysical Research Letters*, *49*(6), e2021GL095774. https://doi.org/10.1029/2021gl095774

Knaff, J. A., Sampson, C. R., & Musgrave, K. D. (2018). An operational rapid intensification prediction aid for the western North Pacific. *Weather Forecasting*, *33*(3), 799–811. https://doi.org/10.1175/waf-d-18-0012.1

Knapp, K. R., Diamond, H. J., Kossin, J. P., Kruk, M. C., & Schreck, C. J. (2018). International best track archive for climate Stewardship (IBTrACS) project, version 4 [dataset]. *NOAA National Centers for Environmental Information*. https://doi.org/10.25921/82ty-9e16

Knapp, K. R., Kruk, M. C., Levinson, D. H., Diamond, H. J., & Neumann, C. J. (2010). The International best track archive for climate Stewardship (IBTrACS). *Bulletin of American Meteorological Society*, *91*(3), 363–376. https://doi.org/10.1175/2009bams2755.1

Kossin, J. P. (2018). A global slowdown of tropical-cyclone translation speed. *Nature*, *558*(7708), 104–107. https://doi.org/10.1038/s41586-018-0158-3

Lanzante, J. R. (2019). Uncertainties in tropical-cyclone translation speed. *Nature*, *570*(7759), E6–E15. https://doi.org/10.1038/s41586-019-1223-2

Lee, C. Y., Tippett, M. K., Sobel, A. H., & Camargo, S. J. (2016). Rapid intensification and the bimodal distribution of tropical cyclone intensity. *Nature Communications*, *7*(1), 10625. https://doi.org/10.1038/ncomms10625

Li, Y., Tang, Y., Wang, S., Toumi, R., Song, X., & Wang, Q. (2023). Recent increases in tropical cyclone rapid intensification events in global offshore regions. *Nature Communications*, *14*(1), 5167. https://doi.org/10.1038/s41467-023-40605-2

Lin, I. –I., Chen, C. –H., Pun, I. –F., Liu, W. T., & Wu, C. –C. (2009). Warm ocean anomaly, air sea fluxes, and the rapid intensification of tropical cyclone Nargis (2008). *Geophysical Research Letters*, *36*(3), L03817. https://doi.org/10.1029/2008gl035815

Lin, I. –I., Pun, I. –F., & Wu, C. –C. (2009). Upper-ocean thermal structure and the western North Pacific category 5 typhoons. Part II: Dependence on translation speed. *Monthly Weather Review*, *137*(11), 3744–3757. https://doi.org/10.1175/2009mwr2713.1

Ma, Z., Fei, J., Lin, Y., & Huang, X. (2020). Modulation of clouds and rainfall by tropical cyclone's cold wakes. *Geophysical Research Letters*, *47*(17), e2020GL088873. https://doi.org/10.1029/2020gl088873

Mei, W., & Pasquero, C. (2013). Spatial and temporal characterization of sea surface temperature response to tropical cyclones. *Journal of Climate*, *26*(11), 3745–3765. https://doi.org/10.1175/jcli-d-12-00125.1

19448007, 2024, 18, Downloaded from https://agupubs.onlinelibrary.wiley.com/doi/10.1029/2024GL110220, Wiley Online Library on [12/02/2025]. See the Terms and Conditions (https://onlinelibrary.wiley.com/terms-and-conditions) on Wiley Online Library for rules of use; OA articles are governed by the applicable Creative Commons License

Mei, W., Pasquero, C., & Primeau, F. (2012). The effect of translation speed upon the intensity of tropical cyclones over the tropical ocean. *Geophysical Research Letters*, *39*(7), L07801. https://doi.org/10.1029/2011gl050765

Moon, I. J., Kim, S. H., & Chan, J. C. L. (2019). Climate change and tropical cyclone trend. *Nature*, *570*(7759), E3–E5. https://doi.org/10.1038/s41586-019-1222-3

Price, J. F., Morzel, J., & Niiler, P. P. (2008). Warming of SST in the cool wake of a moving hurricane. *Journal of Geophysical Research*, *113*(C7), C07010. https://doi.org/10.1029/2007jc004393

Rayner, N. A., Parker, D. E., Horton, E. B., Folland, C. K., Alexander, L. V., Rowell, D. P., et al. (2003). Global analyses of sea surface temperature, sea ice, and night marine air temperature since the late nineteenth century. *Journal of Geophysical Research*, *108*(D14), 4407. https://doi.org/10.1029/2002jd002670

Sasaki, H., Kida, S., Furue, R., Aiki, H., Komori, N., Masumoto, Y., et al. (2020). A global eddying hindcast ocean simulation with OFES2. *Geoscientific Model Development Discussions*, *13*(7), 3319–3336. https://doi.org/10.5194/gmd-13-3319-2020

Shimada, U., Yamaguchi, M., & Nishimura, S. (2020). Is the number of tropical cyclone rapid intensification events in the western North Pacific increasing? *SOLA*, *16*(0), 1–5. https://doi.org/10.2151/sola.2020-001

Shu, S., Ming, J., & Chi, P. (2012). Large-scale characteristics and probability of rapidly intensifying tropical cyclones in the western North Pacific basin. *Weather Forecasting*, *27*(2), 411–423. https://doi.org/10.1175/waf-d-11-00042.1

Song, J., Duan, Y., & Klotzbach, P. J. (2020). Increasing trend in rapid intensification magnitude of tropical cyclones over the western North Pacific. *Environmental Research Letters*, *15*(8), 084043. https://doi.org/10.1088/1748-9326/ab9140

Song, J., Klotzbach, P. J., & Duan, Y. (2021). Increasing lifetime maximum intensity of rapidly intensifying tropical cyclones over the western North Pacific. *Environmental Research Letters*, *16*(3), 034002. https://doi.org/10.1088/1748-9326/abdbf1

Sun, J., Zuo, J., Ling, Z., & Yan, Y. (2016). Role of ocean upper layer warm water in the rapid intensification of tropical cyclones: A case study of typhoon Rammasun (1409). *Acta Oceanologica Sinica*, *35*(3), 63–68. https://doi.org/10.1007/s13131-015-0761-1

Sun, Y., Zhong, Z., Li, T., Yi, L., & Shen, Y. (2021). The slowdown tends to be greater for stronger tropical cyclones. *Journal of Climate*, *34*, 5741–5751. https://doi.org/10.1175/jcli-d-20-0449.1

Walker, N. D., Leben, R. R., Pilley, C. T., Shannon, M., Herndon, D. C., Pun, I. –F., et al. (2014). Slow translation speed causes rapid collapse of northeast Pacific Hurricane Kenneth over cold core eddy. *Geophysical Research Letters*, *41*(21), 7595–7601. https://doi.org/10.1002/2014gl061584

Wang, B., & Zhou, X. (2008). Climate variation and prediction of rapid intensification in tropical cyclones in the western North Pacific. *Meteorology and Atmospheric Physics*, *99*(1–2), 1–16. https://doi.org/10.1007/s00703-006-0238-z

Wang, C., Wu, L., Lu, J., Liu, Q., Zhao, H., Tian, W., & Cao, J. (2020). Interannual variability of the basinwide translation speed of tropical cyclones in the western North Pacific. *Journal of Climate*, *33*(20), 8641–8650. https://doi.org/10.1175/jcli-d-19-0995.1

Wang, G., Zhao, B., Qiao, F., & Zhao, C. (2018). Rapid intensification of super typhoon Haiyan: The important role of a warm-core ocean eddy. *Ocean Dynamics*, *68*(12), 1649–1661. https://doi.org/10.1007/s10236-018-1217-x

Wang, X., Wang, C., Zhang, L., & Wang, X. (2015). Multidecadal variability of tropical cyclone rapid intensification in the western North Pacific. *Journal of Climate*, *28*(9), 806–3820. https://doi.org/10.1175/jcli-d-14-00400.1

Wang, Y., & Wu, C. –C. (2004). Current understanding of tropical cyclone structure and intensity changes—A review. *Meteorology and Atmospheric Physics*, *87*(4), 257–278. https://doi.org/10.1007/s00703-003-0055-6

Wu, K., Wang, C., Wu, L., Zhao, H., & Cao, J. (2022). Slowdown in landfalling tropical cyclone motion in south China. *Geophysical Research Letters*, *49*(21), e2022GL100428. https://doi.org/10.1029/2022gl100428

Wu, L., Wang, R., & Feng, X. (2018). Dominant role of the ocean mixed layer depth in the increased proportion of intense typhoons during 1980–2015. *Earth's Future*, *6*(11), 1518–1527. https://doi.org/10.1029/2018ef000973

Yamaguchi, M., Chan, J. C. L., Moon, I. –J., Yoshida, R., & Mizuta, R. (2020). Global warming changes tropical cyclone translation speed. *Nature Communications*, *11*(1), 47. https://doi.org/10.1038/s41467-019-13902-y

Yesubabu, V., Kattamanchi, V. K., Vissa, N. K., Dasari, H. P., & Sarangam, V. B. R. (2020). Impact of ocean mixed-layer depth initialization on the simulation of tropical cyclones over the Bay of Bengal using the WRF-ARW model. *Meteorological Applications*, *27*(1), e1862. https://doi.org/10.1002/met.1862

Zhang, D., Zhang, J., Shi, L., & Yao, F. (2020). Interdecadal changes of characteristics of tropical cyclone rapid intensification over western North Pacific. *IEEE Access*, *8*, 15781–15791. https://doi.org/10.1109/access.2020.2965976

Zhang, G., Murakami, H., Knutson, T. R., Mizuta, R., & Yoshida, K. (2020). Tropical cyclone motion in a changing climate. *Science Advances*, *6*(17), eaaz7610. https://doi.org/10.1126/sciadv.aaz7610

Zhang, H., He, H., Zhang, W. –Z., & Tian, D. (2021). Upper ocean response to tropical cyclones: A review. *Geoscience Letters*, *8*, 1. https://doi.org/10.1186/s40562-020-00170-8

Zhang, Y., Han, K., Sun, Y., Lin, Y., Zhai, P., Guo, X., & Zhong, W. (2024). Impact of ocean mixed layer depth on tropical cyclone characteristics: A numerical investigation. *Frontiers in Marine Science*, *11*, 1395492. https://doi.org/10.3389/fmars.2024.1395492

Zhao, X., & Chan, J. L. (2017). Changes in tropical cyclone intensity with translation speed and mixed-layer depth: Idealized WRF-ROMS coupled model simulations. *Quarterly Journal of Royal Meteorological Society*, *143*, 152–163. https://doi.org/10.1002/qj.2905

Zuo, H., Balmaseda, M. A., Tietsche, S., Mogensen, K., & Mayer, M. (2019). The ECMWF operational ensemble reanalysis-analysis system for ocean and sea-ice: A description of the system and assessment. *Ocean Science*, *15*(3), 779–808. https://doi.org/10.5194/os-15-779-2019

19448007, 2024, 18, Downloaded from https://agupubs.onlinelibrary.wiley.com/doi/10.1029/2024GL110220, Wiley Online Library on [12/02/2025]. See the Terms and Conditions (https://onlinelibrary.wiley.com/terms-and-conditions) on Wiley Online Library for rules of use; OA articles are governed by the applicable Creative Commons License